

G. Øye
E. Axelrod
Y. Feldman
J. Sjöblom
M. Stöcker

Dielectric properties and Fourier transform IR analysis of MCM-48, Al-MCM-48 and Ti-MCM-48 mesoporous materials

Received: 7 September 1999
Accepted: 10 December 1999

G. Øye · J. Sjöblom
Department of Chemistry
University of Bergen
Allégaten 41 5007 Bergen, Norway

E. Axelrod · Y. Feldman (✉)
Department of Applied Physics
The Hebrew University of Jerusalem
Givat Ram, 91904 Jerusalem, Israel

M. Stöcker
SINTEF Applied Chemistry
P.O. Box 124, Blindern
0314 Oslo, Norway

Abstract Broad-band dielectric spectroscopy was used to investigate the dielectric properties of the mesoporous materials MCM-48, Al-MCM-48 and Ti-MCM-48. The samples were examined in the frequency range from 20 Hz to 1 MHz and in the temperature range from -100 to 250 °C. The dielectric relaxation of the materials has a complex nonexponential behavior with some common features for all the samples. The dielectric spectroscopy and Fourier transform IR measurements identified the relaxation process related to percolation

of H^+ ions associated with silanol groups and water adsorbed in the materials. The non-Debye behavior of the macroscopic dipole correlation functions related to the percolation process allowed us to extract the fractal dimensions of the paths of excitation transfer within the porous medium, and the porosity of each sample was estimated.

Key words Dielectric spectroscopy · FT-IR spectroscopy · Mesoporous materials · MCM-48 · Al-MCM-48 · Ti-MCM-48

Introduction

A new research field was revealed when Mobil Research and Development Corporation reported the synthesis of a new family of mesoporous materials called M41S [1, 2]. Attempts to prepare different materials in the mesoporous range had been made earlier, but the resulting samples were thermally unstable and were catalytically inactive materials [3–5]. The M41S family can be divided into three main groups: MCM-41, which has a one-dimensional, hexagonally ordered pore structure, MCM-48, which has a three-dimensional, cubic pore structure and MCM-50, which has a thermally unstable lamellar structure.

MCM-41 and MCM-48 are characterized by high thermal stability, large surface areas and a uniform pore size distribution. So far, MCM-41 materials have attracted far more interest than MCM-48 materials, probably due to their wider synthesis regime; however, MCM-48 materials have a three-dimensional pore structure, which should make them more applicable

as catalysts and adsorbents due to fewer pore-plugging problems.

In order to make the materials catalytically active, other elements have to be incorporated into the siliceous framework. Acid catalysts are obtained when Al is incorporated into the framework. These types of materials have been tested in several petroleum refining processes [6–10]. Incorporation of Ti or V into the wall structure results in redox catalysts. These materials have turned out to be good catalysts for liquid-phase oxidation processes [11, 12].

Naturally, incorporation of different elements in the framework will give different surface properties of the materials. The variations in the surface properties will also influence the behavior and structural properties of species present in the pores. These phenomena have been studied using various experimental techniques [13–18]. Dielectric spectroscopy is a method well suited to these kinds of studies. The response is affected both by the morphology of the porous materials and by the type of molecules in the pores; hence, the effect of the pore

architecture on the structure and dynamics of the adsorbed species can be studied.

In the present work the dielectric relaxation properties of MCM-48, Al-MCM-48 and Ti-MCM-48 (with two different Si/Ti molar ratios) are studied over wide temperature and frequency ranges. The dielectric relaxation assigned to percolation in the samples is of particular interest. By combining the results from the dielectric measurements and those from diffuse reflectance Fourier transform (FT)-IR spectroscopy the percolating species can be identified.

Experimental

Syntheses of the materials

MCM-48

The synthesis was undertaken according to the following procedure [19]. Cetyltrimethylammonium bromide (CTAB) and NaF were dissolved in distilled water. This solution was then stabilized at 35–40 °C.

Tetraethoxysilane (TEOS) was added to a solution consisting of NaOH dissolved in distilled water. This solution was stirred vigorously for 5 min before it was added to the structure-directing solution. The resulting solution was stirred for 15 min and was then transferred to a Teflon bottle and heated under static conditions at 100 °C. The molar composition of the solution was 1.0 CTAB:1.6 TEOS:0.2 NaF:0.8 NaOH:97 H₂O.

After 72 h the samples were cooled to room temperature. The as-synthesized solid was recovered by filtration and was thoroughly washed with distilled water. The solid was dried at ambient temperature. The template was removed by calcination at 540 °C under flowing nitrogen for 1 h, followed by 6 h under flowing air.

Al-MCM-48

The aluminum-containing materials were synthesized according to the following procedure [20]. CTAB was dissolved in distilled water and NaOH was added. The temperature of this solution was stabilized at approximately 36 °C before addition of TEOS. After 5 min of stirring, aluminum sulfate was added. Then the solution

was stirred for 55 min before it was transferred to a Teflon bottle and kept at 100 °C for 72 h.

The molar composition of the solution was 1.0 CTAB:2.5 TEOS:1.5 NaOH:0.04 aluminum sulfate:244 H₂O. Before calcination the samples were washed with distilled water and dried at ambient temperature.

The calcination was preceded by a template extraction procedure. Ammonium nitrate (1 g) and sample (1 g) were dissolved in 100 ml hot ethanol. The mixture was refluxed under stirring for 24 h before the solvent was filtered off. This procedure was repeated. Finally, the sample was calcined at 540 °C for 5 h in flowing air.

Ti-MCM-48 [21]

The Ti-MCM-48 samples were prepared with Si/Ti molar ratios in the synthesis solutions of approximately 40 and 5. These samples are from now on called Ti-40 and Ti-5, respectively. The syntheses were performed as follows. CTAB and NaOH were dissolved in distilled water. The temperature of the solution was stabilized at about 35 °C before TEOS was added. TEOS was allowed to react for 5 min before addition of tetraethyl orthotitanate (TEOT) in appropriate amounts. Then the solution was mixed for 20 min. The molar ratio in the synthesis solution was 1.0 CTAB:0.8 NaOH:97 H₂O:1.6 (TEOS + TEOT).

Finally, the solutions were transferred to Teflon bottles and sealed. They were kept at 100 °C under static conditions for 2.5–3 days. Then the as-synthesized solids were recovered by filtration, washed with distilled water and dried at ambient temperature. The samples were calcined at 540 °C for 2 h under flowing N₂, followed by 6 h under flowing air.

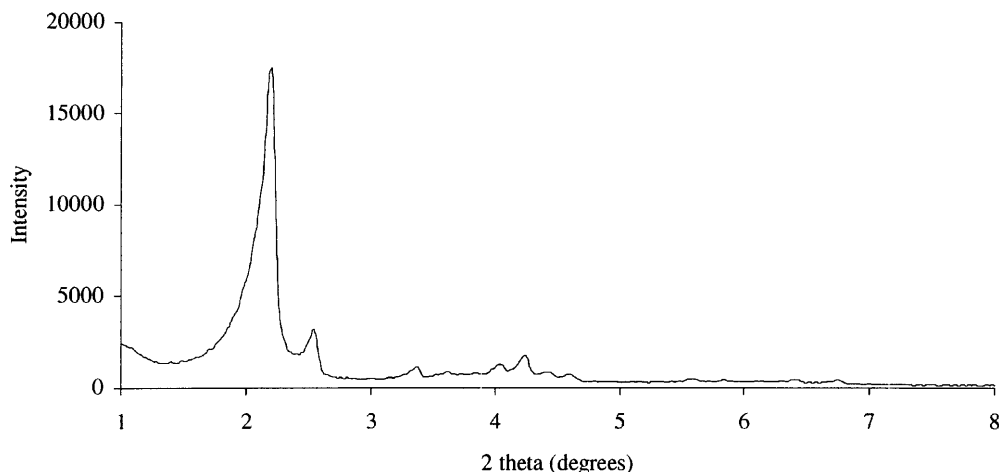
Experimental techniques

Dielectric spectroscopy

Dielectric measurements in the frequency range from 20 Hz to 1 MHz were performed using a BDS 4284 (NOVOCONTROL) broad-band dielectric spectrometer with automatic temperature control by a QUATRO Cryosystem. The accuracy of the measured dielectric permittivity and the dielectric losses is estimated to be better than 3% [22].

The measurements were carried out in the following way. Each of the samples was placed into the sample cell, consisting of two parallel capacitor plates, at room temperature. The measurements were then performed by cooling the samples from 20 to –100 °C. In the second stage the samples were measured while heating them to

Fig. 1 The powder X-ray diffraction pattern of the MCM-48 sample



250 °C. Then the samples were measured with the temperature reduced to 20 °C. A step of 5 °C was used over the whole temperature range.

Diffuse-reflectance FT-IR spectroscopy

The FT-IR measurements were performed using a Nicolet 800 FT-IR spectrometer applying a medium-band MCT detector and a Spectra-Tech diffuse-reflectance cell. The optical resolution was 4 cm⁻¹ and 16 scans were carried out for each measurement. The samples were prepared as KBr pellets, containing approximately 5 wt% sample. Pure KBr was used as a reference.

Results and discussion

The X-ray diffraction (XRD) pattern of calcined MCM-48 is shown in Fig. 1. The reflection peaks can be indexed according to the *Ia3d* space group, which confirms a cubic ordered pore structure. The XRD patterns of the other samples look similar.

Typical spectra of the dielectric permittivity and the dielectric losses as a function of frequency and temperature for sample Ti-5 are given in Fig. 2. The whole temperature range of dielectric relaxation behavior in the samples under investigation can be described in terms of two or three distributed relaxation processes (depending on the sample) and they have some common features. The $\epsilon''(f, T)$ cuts at a constant frequency plane (1 kHz) for all the samples under study represent the temperature dependence of the dielectric losses during heating from -100 to 250 °C (Fig. 3). One can see that in the low-frequency region and in the temperature interval of 0–100 °C some relaxation process can be detected for all the samples. The amplitude of this process essentially decreases when the frequency increases (Fig. 2a) and the maximum of the dielectric losses (Fig. 2b) has almost no temperature dependence. The largest amplitude is observed for the Ti-40 sample and the smallest one is for MCM-48 (Fig. 3). In this article we will mainly concentrate on the study of this process, which is a typical dielectric response for percolation behavior [16, 23]. An analysis of the parameters of this relaxation process allowed us to determine morphological properties of the samples, such as fractal dimension (D_f) and porosity (ϕ) [16]. The dielectric response for this process in the time domain can be described by the Kohlrausch–Williams–Watts (KWW) expression:

$$\Psi(t/\tau) \sim \exp[-(t/\tau)^\nu], \quad (1)$$

where Ψ is the dipole correlation function, τ is the average relaxation time and ν is the stretched parameter, $0 < \nu \leq 1$. It was shown [24, 25] that in complex fractal systems, for the relaxation related to the charge transfer along the ramified path, ν can be related to the D_f of the path,

$$\nu = D_f/3. \quad (2)$$

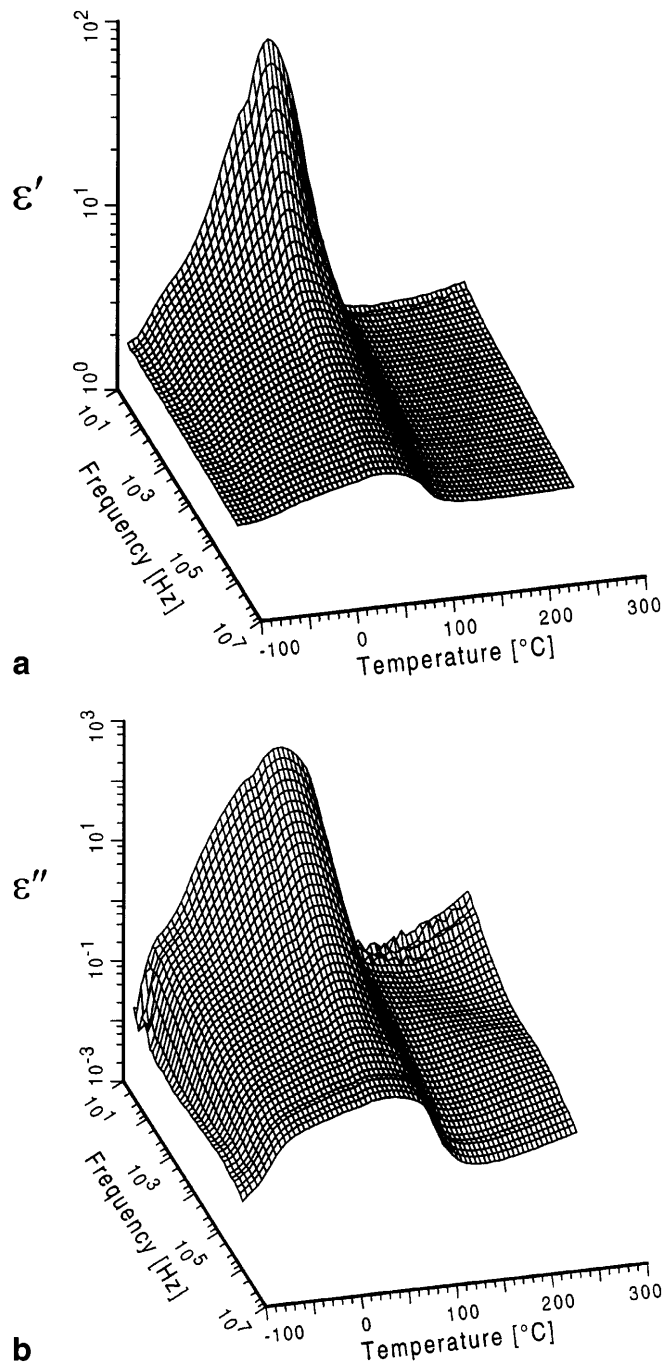


Fig. 2 Three dimensional plot of the frequency and temperature dependence of the dielectric **a** permittivity, ϵ' , and **b** dielectric losses, ϵ'' , for the sample Ti-5

In order to describe the porous medium, the relationship between D_f and ϕ of the material was obtained using the model of a random fractal [26]. In the simplest case of the model, the mean deviations of the scaling parameters of the random fractal from the scaling parameters of the regular dominating fractal are zero. This makes it

Fig. 3 Temperature dependence of the 1 kHz frequency behavior of ε'' of all the samples

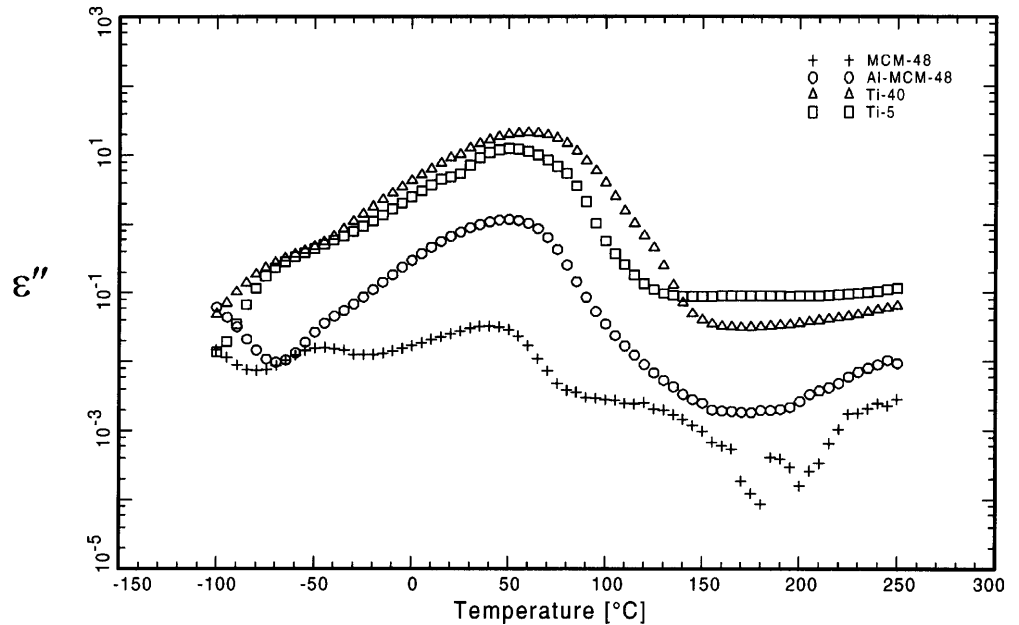


Table 1 Values of fractal dimension, D_f , and porosity, ϕ , for all the mesoporous samples measured

Sample	Stretched parameter ν	D_f	ϕ (%) (obtained from dielectric measurements)	ϕ (%) (obtained from loss of mass during calcination)
MCM-48	0.83 ± 0.02	2.49 ± 0.06	66 ± 1	68 ± 1
Al-MCM-48	0.68 ± 0.02	2.04 ± 0.06	51 ± 1	52 ± 1
Ti-40	0.89 ± 0.02	2.67 ± 0.06	75 ± 1	73 ± 1
Ti-5	0.91 ± 0.02	2.73 ± 0.06	79 ± 1	50 ± 1

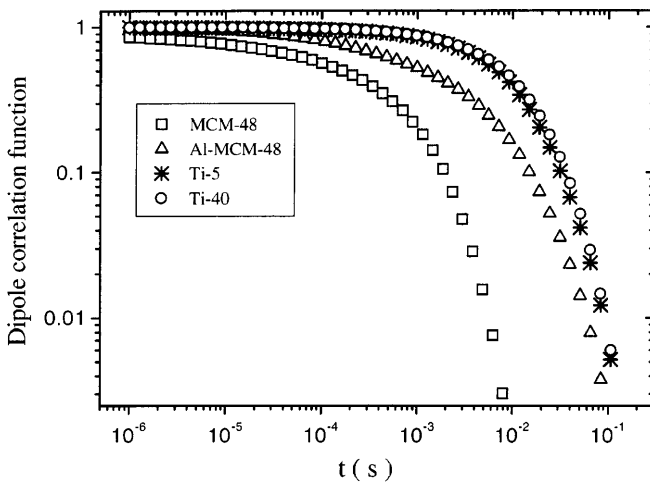


Fig. 4 Macroscopic dipole correlation functions of all the samples

possible to obtain the approximate relationship between ϕ and D_f of the porous structure:

$$\phi = \frac{1}{4 - D_f} \frac{1 - \mu^{4-D_f}}{1 - \mu} \approx \frac{1}{4 - D_f} \quad (3)$$

where $\mu = \lambda/\Lambda$, where Λ coincides with the upper and λ with the lower limit (resolution of measuring setup) of the self-similarity.

The experimental macroscopic dipole correlation functions for all the samples at the temperature of the maximum dielectric strength (40 °C for MCM-48, 50 °C for Al-MCM-48, 45 °C for Ti-5 and 60 °C for Ti-40) were obtained from the inverse Fourier transform (Fig. 4). The correlation functions were fitted by the sum of two KWW processes. The parameter ν for the long relaxation process was used for the calculation of D_f . The results of the calculations are presented in Table 1. This table also reveals the values of the porosity determined from the dipole correlation function analysis. As one can see, they are in good agreement with the values of the porosity determined from the loss of mass during calcination (calculated by weighing the samples before and after calcination) for all the samples, except sample Ti-5. It is, however, important to note that the samples treated in this work are powdered samples and percolation will also occur in voids between the packed particles. FT-IR measurements (see later) show that the Ti-5 sample contains a relatively large amount of (bulk) water. A higher extent

of the percolation may therefore occur in the interparticle voids. This can explain the difference between the porosity values obtained from the loss of mass during calcination and the apparent porosity calculated from the dielectric measurements.

Diffuse-reflectance FT-IR spectroscopy was utilized to investigate the mesoporous samples. The diffuse reflectance FT-IR spectrum of Al-MCM-48 is shown in Fig. 5. A narrow, low-intensity vibrational band is seen at approximately 3743 cm^{-1} . This is assigned to free terminal silanol groups. The broad band ranging from about 3700 to 3000 cm^{-1} is associated with hydrogen-bonded groups. Traces of hydrocarbons are also seen at the shoulder of this band (around 2900 cm^{-1}). The band from about 1700 to 1600 cm^{-1} corresponds to the bending mode of water. This suggests that water is adsorbed in the sample. The band at 3700 – 3000 cm^{-1} may then originate from hydrogen bonds between silanol groups, between silanol groups and water and between water molecules. Similar results are found for the Ti-MCM-48 samples [21].

MCM-48 differs from the other samples. As shown in Fig. 6, no bands corresponding to hydrogen-bonded species or water bending are present. The narrow band assigned to terminal silanol groups is, however, seen at approximately 3746 cm^{-1} . Consequently, the surface mainly consists of isolated silanol groups. Furthermore, previous studies showed that MCM-48 samples have significantly larger surface areas (about $1300\text{ m}^2/\text{g}$ [19]) compared to the Ti-5 sample, ($742\text{ m}^2/\text{g}$ [21]).

These results may indicate the origin of the observed relaxation processes related to percolation. The FT-IR results and the large surface area suggest that water is virtually absent in MCM-48. Consequently, the relaxation process seems primarily to be due to the percolation of H^+ ions associated with the silanol groups and its amplitude is low. The presence of water in the Al-MCM-48 and Ti-MCM-48 samples is confirmed by the FT-IR results. This can also account for the relatively low surface area found for the Ti-5 sample. The higher amplitude of the relaxation process in these samples can, thereby, be explained by additional contributions from percolation of the adsorbed water. Furthermore, it is tempting to suggest that the Ti-MCM-48 samples contain more adsorbed water than Al-MCM-48, since these show the highest amplitude of the two.

An additional relaxation process is observed for MCM-48 and Al-MCM-48 at low temperatures (Fig. 3). The amplitude of the process increases with increasing frequencies. It is well known that water close to surfaces behaves differently from bulk water, and in previous studies of similar relaxation processes these have been attributed to the dynamics of mobile species interacting with the surface [25]. It has also been suggested that water molecules reorient into icelike structures [13]. Furthermore, water-saturated mesoporous materials have been studied by means of ^1H NMR spectroscopy [27–32]. The signal intensity and spin-lattice relaxation times were studied as a function of temperature. Several states of the water molecules were identified, and the

Fig. 5 Diffuse-reflectance Fourier transform (FT)-IR spectrum of the Al-MCM-48 sample

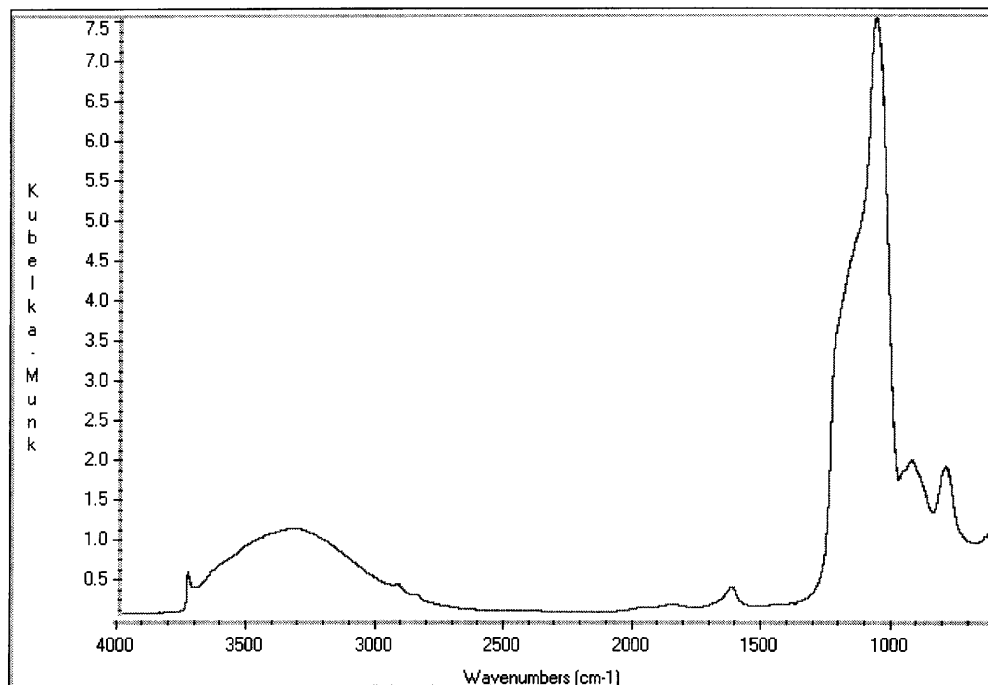
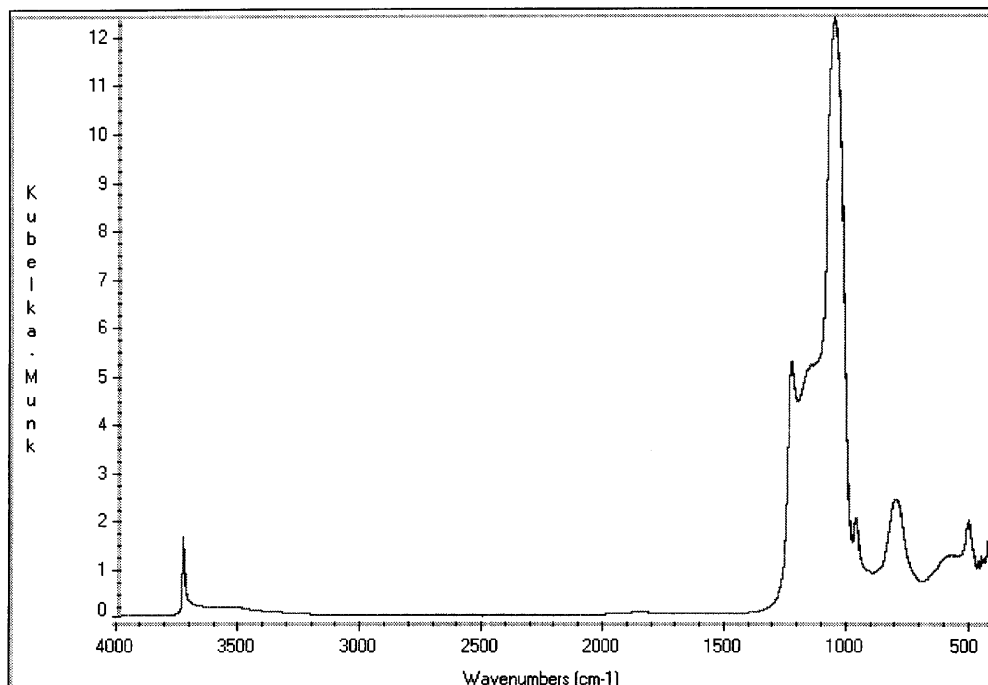


Fig. 6 Diffuse-reflectance FT-IR spectrum of the MCM-48 sample



freezing-point or melting-point transition data of the confined water were applied to estimate the pore size distribution, the specific surface area and the relative distribution of pore volumes of the materials [32]. This process seems to be comparable to the one observed in the dielectric measurements, and possibly closer investigations of this relaxation process may give similar information.

Conclusions

The dielectric behavior of mesoporous materials with cubic ordered pore structures was investigated. The experiments were carried out for purely siliceous materials and for materials containing Al or Ti in the wall structure as well. Analysis of a dielectric relaxation process, corresponding to percolation of charged spe-

cies, made it possible to estimate the porosity of the samples. For most of the samples, these results agreed quite well with the porosity estimated from mass losses during calcination. FT-IR and N₂ adsorption-desorption results revealed that the percolating species were mainly H⁺ ions associated with silanol groups and adsorbed water.

A low-temperature relaxation process was found for MCM-48 and Al-MCM-48. A closer analysis of this process is necessary in order to extract reliable information from it. Possibly, structural and dynamic properties of the surface species could be obtained by such an analysis. Analogous to the reported ¹H NMR investigations, characterization of the pore structure could be possible as well.

Acknowledgements G. Ø. thanks the Norwegian Research Council (NFR) for a Dr. Scient. grant. The FT-IR spectrometer was also financed by NFR.

References

1. Beck JS, Vartuli JC, Roth WJ, Leonowicz ME, Kresge CT, Schmitt KD, Chu CT-W, Olson DH, Sheppard EW, McCullen SB, Higgins JB, Schlenker J (1992) *J Am Chem Soc* 114:10834
2. Kresge CT, Leonowicz ME, Roth WJ, Vartuli JC, Beck JS (1992) *Nature* 359:710
3. Wilson ST, Lok BM, Messina CA, Cannan TR, Flanigen EM (1982) *J Am Chem Soc* 104:1146
4. Davis ME, Saldarriaga C, Montes C, Garces J, Crowder C (1988) *Nature* 331:698
5. Jones RH, Thomas JM, Chen J, Xu R, Huo Q, Li S, Ma Z, Chippindale AM (1993) *J Solid State Chem* 102:204
6. Corma A, Martínez-Soria A, Mortón JB (1995) *J Catal* 153:25
7. Kim JB, Inui T (1996) *Catal Lett* 36:103
8. Mokaya R, Jones W, Luan Z, Alba MD, Klinowski J (1996) *Catal Lett* 37:113
9. Girgis MJ, Tsao YP (1996) *Ind Eng Chem Res* 35:386
10. Roos K, Liepold A, Reschtilowski W, Schmidt R, Karlsson A, Stöcker M (1995) *Stud Surf Sci Catal* 94:389
11. Gontier S, Tuel A (1995) *Stud Surf Sci Catal* 97:157

-
12. Gontier S, Tuel A (1996) *J Catal* 157:124
 13. Pissis P, Laudat J, Daoukaki D, Kyritsis A (1994) *J Non-Cryst Solids* 171:201
 14. Schüller J, Richert R, Fisher EW (1995) *Phys Rev B* 52:15232
 15. Arndt M, Stannarius R, Gorbatschow W, Kremer F (1996) *Phys Rev E* 54:5377
 16. Gutina A, Axelrod E, Puzenko A, Rysiakiewicz-Pasek E, Kozlovich N, Feldman Y (1998) *J Non-Cryst Solids* 235:302
 17. Ozeki S, Masuda Y, Sano H (1989) *J Phys Chem* 93:7226
 18. Overloop K, van Gerven L (1993) *J Magn Reson* 101:179
 19. Øye G, Sjöblom J, Stöcker M (1999) *Microporous Mesoporous Mater* 27:171
 20. Schmidt R, Junggreen H, Stöcker M (1996) *Chem Commun* 7:875
 21. Øye G, Sjöblom J, Stöcker M (2000) *J Dispersion Sci Technol* 21:49
 22. Schamburg G (1997) *Dielectric Newsletter* 8:5
 23. Feldman Y, Kozlovich N, Nir I, Garti N (1995) *Phys Rev E* 51:478–491
 24. Feldman Y, Kozlovich N, Alexandrov Y, Nigmatullin R, Ryabov Y (1996) *Phys Rev E* 54:5420
 25. Gutina A, Haruvy Y, Gilath I, Axelrod E, Kozlovich N, Feldman Y J (1999) *Phys Chem B* 103:5454
 26. Nigmatullin R (1989) *Phys Status Solid B* 153:49
 27. Akporiaye D, Hansen EW, Schmidt R, Stöcker M (1994) *J Phys Chem* 98:1926
 28. Schmidt R, Stöcker M, Hansen EW, Akporiaye D, Ellestad OH (1995) *Microporous Mater* 3:443
 29. Hansen EW, Schmidt R, Stöcker M, Akporiaye D (1995) *J Phys Chem* 99:4148
 30. Schmidt R, Hansen EW, Stöcker M, Akporiaye D, Ellestad OH (1995) *J Am Chem Soc* 117:4049
 31. Hansen EW, Schmidt R, Stöcker M (1996) *J Phys Chem* 100:11396
 32. Hansen EW, Tangstad E, Myrvold E, Myrstad T (1997) *J Phys Chem* 101:10709